Universiteit Leiden
The Netherlands

Structural connectivity of dopaminergic pathways in major depressive disorder: an ultra-high resolution 7-Tesla diffusion MRI study.

Liu, W.; Heij, J.; Liu, S.; Liebrand, L.; Caan, M.; Zwaag, W. van der; ... ; Wingen, G. van

Citation
Liu, W., Heij, J., Liu, S., Liebrand, L., Caan, M., Zwaag, W. van der, ... Wingen, G. van. (2024). Structural connectivity of dopaminergic pathways in major depressive disorder: an ultra-high resolution 7-Tesla diffusion MRI study. *European Neuropsychopharmacology, 89*, 58-70. doi:10.1016/j.euroneuro.2024.07.014

Version:	Publisher's Version
License:	Creative Commons CC BY 4.0 license
Downloaded from:	https://hdl.handle.net/1887/4209588

Note: To cite this publication please use the final published version (if applicable).

European Neuropsychopharmacology 89 (2024) 58–70

Contents lists available at ScienceDirect

European Neuropsychopharmacology

journal homepage: www.sciencedirect.com/journal/european-neuropsychopharmacology

Structural connectivity of dopaminergic pathways in major depressive disorder: An ultra-high resolution 7-Tesla diffusion MRI study

Weijian Liu [a,b,c], Jurjen Heij [d,e], Shu Liu [l], Luka Liebrand [b,f], Matthan Caan [b,g], Wietske van der Zwaag [d,e], Dick J Veltman [h], Lin Lu [c,i,j], Moji Aghajani [h,k,†], Guido van Wingen [a,b,†,*]

[a] Amsterdam UMC location University of Amsterdam, Department of Psychiatry, Amsterdam, the Netherlands
[b] Amsterdam Neuroscience, Amsterdam, the Netherlands
[c] Peking University Sixth Hospital, Peking University Institute of Mental Health, NHC Key Laboratory of Mental Health (Peking University), National Clinical Research Center for Mental Disorders (Peking University Sixth Hospital), Peking University, Beijing, China
[d] Spinoza Centre for Neuroimaging, KNAW, Amsterdam, the Netherlands
[e] Netherlands Institute for Neuroscience, Amsterdam, Netherlands
[f] Amsterdam UMC location Vrije Universiteit Amsterdam, Department of Radiation Oncology, Amsterdam, the Netherlands
[g] Amsterdam UMC location University of Amsterdam, Department of Biomedical Engineering & Physics, Amsterdam, the Netherlands
[h] Amsterdam UMC location Vrije Universiteit Amsterdam, Department of Psychiatry, Amsterdam, Netherlands
[i] Peking-Tsinghua Centre for Life Sciences and PKU-IDG/McGovern Institute for Brain Research, Peking University, Beijing, China
[j] National Institute on Drug Dependence and Beijing Key Laboratory of Drug Dependence, Peking University, Beijing, China
[k] Institute of Education & Child Studies, Section Forensic Family & Youth Care, Leiden University, the Netherlands
[l] Key Laboratory of Genetic Evolution & Animal Models, National Research Facility for Phenotypic & Genetic Analysis of Model Animals (Primate Facility), National Resource Center for Non-Human Primates, Kunming Institute of Zoology, Chinese Academy of Sciences, Kunming, China

ARTICLE INFO

Keywords:
Ultra-high resolution diffusion MRI
7.0 Tesla
Dopamine pathway
Structural connectivity
Major depressive disorder

ABSTRACT

Accumulating evidence points to imbalanced dopamine (DA) signaling and circulating levels in the pathophysiology of major depressive disorder (MDD). However, the use of conventional MRI scanners and acquisition techniques has prevented a thorough examination of DA neural pathways in MDD. We uniquely employed ultra-high field diffusion MRI at 7.0 Tesla to map the white matter architecture and integrity of several DA pathways in MDD patients. Fifty-three MDD patients and 12 healthy controls (HCs) were enrolled in the final analysis. Images were acquired using a 7.0 Tesla MRI scanner. FreeSurfer was used to segment components of DA pathways, and MRtrix was used to perform preprocessing and tractography of mesolimbic, mesocortical, nigrostriatal, and unconventional DA pathways. Bayesian analyses assessed the impact of MDD and clinical features on DA tracts. MDD was associated with perturbed white matter microstructural properties of the nigrostriatal pathway, while several MDD features (severity of depression/age of onset/insomnia) related to connectivity changes within mesocortical, nigrostriatal, and unconventional pathways. MDD is associated with microstructural differences in the nigrostriatal pathway. The findings provide insight into the structural architecture and integrity of several DA pathways in MDD, and implicate their involvement in the clinical manifestation of MDD.

1. Introduction

Major depressive disorder (MDD) is one of the most severe global public health issues (Belmaker, 2008; World Health Organization, 2008). Despite decades of research, the pathophysiology of MDD remains incompletely understood (Malhi and Mann, 2018; Otte et al., 2016; Pizzagalli et al., 2019). The development and widespread use of the most commonly employed medication class for MDD treatment, selective serotonin reuptake inhibitors (SSRIs) and serotonin-norepinephrine reuptake inhibitors (SNRIs) (Belmaker, 2008; Malhi and Mann, 2018; Otte et al., 2016), revolve around the concept of deficient serotonin and norepinephrine signaling in the brain (Belmaker,

* Corresponding author.
E-mail addresses: w.liu1@amsterdamumc.nl (W. Liu), linlu@bjmu.edu.cn (L. Lu), g.a.vanwingen@amsterdamumc.nl (G. van Wingen).
† Moji Aghajani & Guido van Wingen are shared senior authors.

https://doi.org/10.1016/j.euroneuro.2024.07.014
Received 8 January 2024; Received in revised form 11 July 2024; Accepted 31 July 2024
Available online 27 September 2024
0924-977X/© 2024 The Author(s). Published by Elsevier B.V. This is an open access article under the CC BY license (http://creativecommons.org/licenses/by/4.0/).

2008; Bunney and Davis, 1965; Coppen, 1967; Schildkraut et al., 1965). However, these medications typically require several weeks to take effect (Katz et al., 2004), and about 50%-60% of patients fail to attain a sufficient response after undergoing antidepressant treatment (Fava, 2003). In addition, some evidence even suggests that long-term use of antidepressants may reduce serotonin activity (Bosker et al., 2010; Fava, 2020). The involvement of serotonin mechanisms has been hotly debated. Some studies have revealed that there is no consistent evidence that serotonin is involved in the pathophysiology of depression (Moncrieff et al., 2023). However, there have been rebuttals to this study, arguing that the conclusions have been exaggerated due to flaws in the research method (Jauhar et al., 2023). This suggests that the pathological mechanism of MDD is difficult to explain solely by serotonin and/or norepinephrine deficiency. Therefore, considerable attention is now directed to another candidate neurotransmitter, namely dopamine (DA) (Pizzagalli et al., 2019), which for a long time was overlooked and overshadowed by research focused primarily on serotonin and norepinephrine (Dunlop and Nemeroff, 2007).

DA plays a crucial role in regulating motivation and maintaining the experience of pleasure (Hori and Kunugi, 2013). Deficiency in DA can lead to loss of ability to experience pleasure from normally rewarding stimuli (Russo and Nestler, 2013), which is one of the core symptoms of depression (Dunlop and Nemeroff, 2007). Losing the ability to experience pleasure also frequently persists as a residual symptom in patients after treatment for depression (Belujon and Grace, 2017) and is considered a key factor in the development of treatment-resistant depression (Klein, 1974; McMakin et al., 2012; Pizzagalli, 2022; Vrieze et al., 2013). Clinical evidence shows that DA reuptake inhibitors and DA receptor agonists are effective for treatment-resistant depression (Dunlop and Nemeroff, 2007). Furthermore, evidence from positron emission tomography (PET) imaging revealed a decrease in striatal DA transporter expression in MDD (Pizzagalli et al., 2019), while the severity of depression and the number of suicide attempts both seem to correlate with lower levels of homovanillic acid, a major DA metabolite (Engström et al., 1999; Reddy et al., 1992). As such, it is important to gain more insight into the DA system for a more comprehensive and profound understanding of MDD pathophysiology.

Furthermore, there is growing evidence that depression involves abnormalities in brain circuits (Scheepens et al., 2020), so it is necessary to explore the DA system in depth at the pathway level. The DA system is generally divided into three major pathways: (a) the mesocortical pathway from ventral tegmental area (VTA) to prefrontal cortex; (b) the mesolimbic pathway from VTA to nucleus accumbens (NAcc)/hippocampus (HIP)/amygdala (AMY); and (c) the nigrostriatal pathway from substantia nigra (SN) to the dorsal striatum (Fig. 1) (Belujon and Grace, 2017; Gangadhar and Rao, 2015; Klein et al., 2019; Pariyadath et al.,

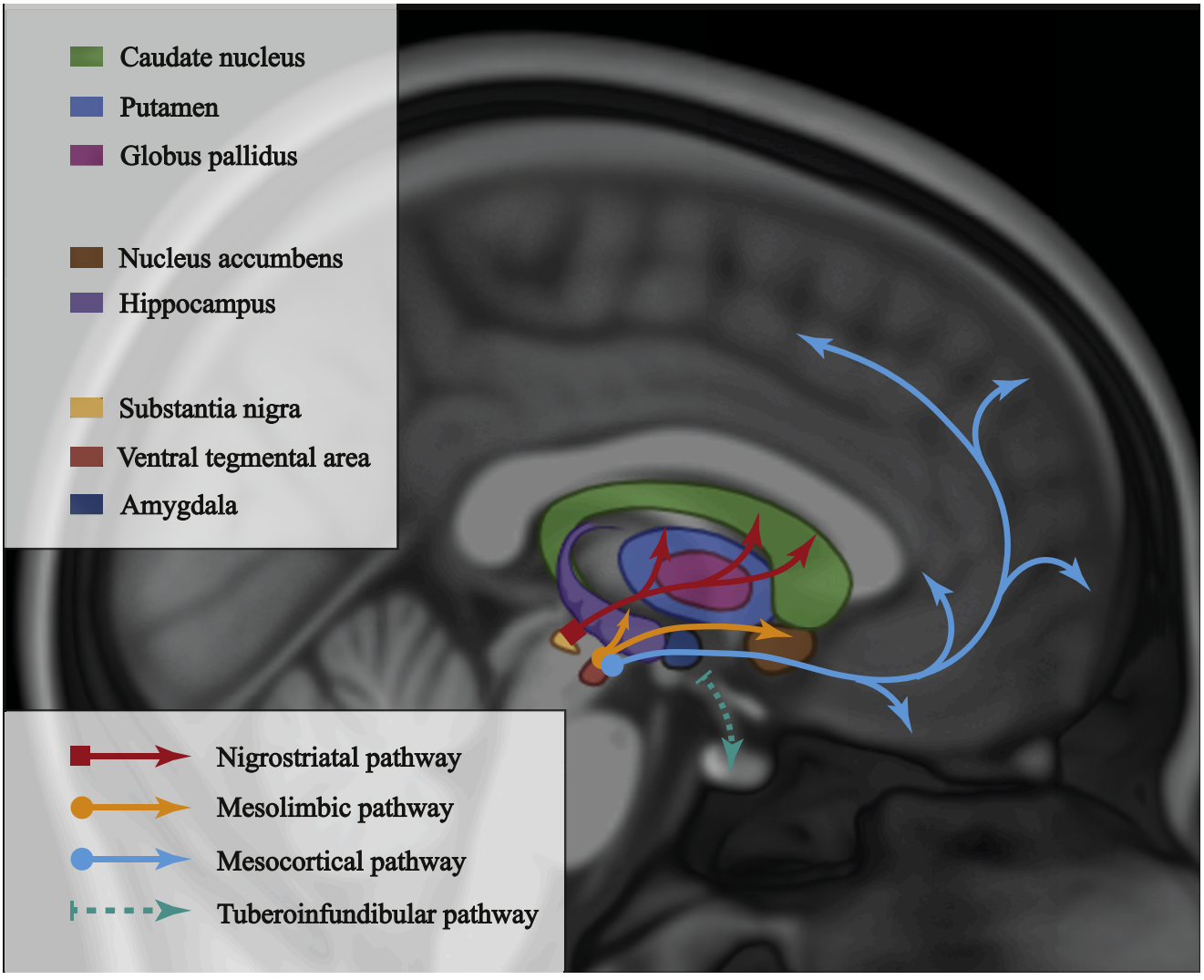

Fig. 1. The main dopamine pathways.
Color coding: red, nigrostriatal pathway; orange, mesolimbic pathway; blue, mesocortical pathway; green, tuberoinfundibular pathway.

2016; Travis, 2003). Diffusion MRI (dMRI) is deemed one of the most reliable and robust methods for in-vivo mapping of white matter neural pathway characteristics (Maier-Hein et al., 2017). However, there is a relative lack of research using dMRI technology to explore the DA pathways in patients with MDD (Bracht et al., 2022). The limited research on white matter differences in DA pathways among individuals with MDD is primarily concentrated on the mesocortical pathway, which is relatively easier to reconstruct than other DA pathways. A study demonstrated that a reduced tract volume of the mesocortical pathway was correlated with greater severity of depressive symptoms and diminished hedonic tone, while a lower streamline count (SC) in the mesocortical pathway was linked to more severe depressive symptoms (Bracht et al., 2022). Another study showed diminished fractional anisotropy (FA) of mesocortical pathway in relation to both MDD diagnosis and severity of depressive symptoms (Bracht et al., 2014). Such disorder-specific shifts in white matter microstructure have so far not been documented for the other DA neural pathways (Bracht et al., 2014). Complex fiber bundle architecture between origins and terminals of certain pathways (e.g., SN-Striatum), along with the small size and indistinct boundaries of some key regions (e.g., VTA), are partly to blame as they complicate reliable pathway reconstruction (Kwon et al., 2021; Theisen et al., 2017; Trutti et al., 2019).

The use of Ultra-High Field (UHF) dMRI at 7.0 Tesla and above is increasingly postulated to overcome these limitations, as the increased signal-to-noise ratio could be exchanged for enhanced spatial resolution (Vu et al., 2015), thus enabling improved segmentation of small deep-lying brain structures and more precise reconstruction of white matter pathways (Liebrand et al., 2020; Strotmann et al., 2014). UHF dMRI moreover greatly enhances the fitting of subsequent data to the diffusion tensor model, thereby reducing uncertainties in diffusion tensor imaging estimates in comparison to standard field strength MRI (1.5/3.0 Tesla) (Polders et al., 2011). Despite these evident benefits, no study has yet utilized UHF dMRI to investigate white matter characteristics of DA pathways in MDD patients. We therefore used the capabilities of UHF dMRI at 7.0 Tesla to uniquely explore the white matter connectivity architecture of DA pathways in MDD. We hypothesized that white matter connectivity of DA pathways is altered in MDD patients, and additionally explored whether clinical variables (medicated condition; episodes; typical subtype; severity of depression, anxiety symptoms, insomnia, childhood trauma; and age of onset) influence DA pathways connectivity characteristics.

2. Method

2.1. Participant recruitment

Patients with MDD recruited in this study met the following inclusion criteria: (1) a primary diagnosis of current MDD that occurred within the last 6 months, according to DSM-5 criteria, as determined by the Composite International Diagnostic Interview (CIDI) (Smeets and Dingemans, 1993); (2) aged between 20-55. HCs met the following inclusion criteria: (1) no history of depression diagnosis or treatment, nor any other psychopathology; (2) normal or subclinical scores on dimensional measures of psychopathology; (3) aged between 20-55. Exclusion criteria for the entire sample: (1) presence of psychoses, mania, Tourette's syndrome, or obsessive-compulsive disorder; (2) diagnosis of major internal or neurological disorders; (3) traumatic head injury; (4) current substance abuse or dependence requiring treatment; (5) evidence of acute suicidal risk requiring immediate intervention; (6) MRI contradictions, including metal implants, heart arrhythmia, or claustrophobia; (7) left-handedness; (8) pregnancy; (9) inadequate understanding of the Dutch language.

After excluding one MDD patient with poor T1-weighted image quality, one MDD patient and one HC with poor diffusion-weighted image (DWI) quality, as well as one HC and two MDD patients who did not have DWI, a total of 53 MDD participants (age = 36.57 ± 10.71 years, 13 males) and 12 HCs (age = 34.37 ± 9.67 years, 5 males) were included in the final analysis. The ethical review board of the Amsterdam UMC (location VUmc) approved this study, and written informed consent was obtained from all participants. Other results from this study are reported elsewhere (Heij et al., 2022).

2.2. Clinical interview and assessment

Clinical interviews and assessments were finished on the same day of MRI scanning. The Inventory for Depressive Symptomatology (IDS) (Rush et al., 1996), the Beck's Anxiety Inventory (BAI) (Beck et al., 1988), the Insomnia Rating Scale (IRS) (Levine et al., 2003), and The Childhood Trauma Questionnaire (CTQ) (de Graaf et al., 2002) were used to measure the severity of depression, anxiety, insomnia, and childhood trauma, respectively. To meet the criteria for atypical MDD, patients needed to have specific scores on various IDS items. Emotional reactivity required scores of 0, 1, or 2, leaden paralysis required scores of 2 or 3, weight gain or increased appetite required scores of 2 or 3, hypersomnia required scores of 2 or 3, and interpersonal sensitivity required a score of 3. Furthermore, to be classified as having atypical MDD, patients had to be emotionally reactive (not scoring 3 on the emotional response item) and meet the criteria for at least 2 of the other 4 symptoms (Novick et al., 2005).

2.3. MRI acquisition

Images were acquired using a Philips Achieva 7.0 Tesla MRI scanner with a 32-channel head array coil. A DWI sequence was used with the following parameters: Echo time (TE) = 74 ms, repetition time (TR) = 11224 ms, field of view (FOV) = 214 × 214 × 126.5 mm, flip angle = 90°, spatial resolution = 1.337 × 1.337 × 1.49 mm, and the number of gradient directions = 64. The b-value for the sequence was 1200 s/mm^2, and one b = 0 s/mm^2 was acquired. Additionally, two DWI reverse phase-encoding direction scans were acquired to correct for gradient distortions (Andersson and Sotiropoulos, 2016). T1 weighted images were obtained as anatomical reference using an MP2RAGEME (multi--echo magnetization-prepared rapid gradient echo) sequence (Caan et al., 2019). The MP2RAGEME is an extension of the MP2RAGE sequence (Marques et al., 2010) and consists of two rapid gradient echo ($GRE_{1,2}$) images that are acquired after a 180° degrees inversion pulse and excitation pulses with inversion times $TI_{1,2}$ = [670 ms, 3675.4 ms]. A multi-echo readout was used in the second inversion, with four equally spaced echo times (TE_1= 3 ms, $TE_{2,1-4}$ = 3, 11.5, 19, 28.5 ms). Other scan parameters include flip angles$_{1,2}$ = [4°, 4°]; $TR_{GRE1,2}$ = [6.2 ms, 31 ms]; bandwidth = 404.9 MHz; $TR_{MP2RAGEME}$ = 6778 ms; acceleration factor $SENSE_{PA}$ = 2; FOV = 205 × 205 × 164 mm; acquired voxel size = 0.7 × 0.7 × 0.7 mm; acquisition matrix was 292 × 290; reconstructed voxel size 0.64 × 0.64 × 0.7 mm; turbo factor (TFE) = 150, resulting in 176 shots; Total acquisition time = 19.53 minutes.

2.4. Structural data preprocessing

T1-weighted images were processed with FreeSurfer version 7.2.0 "recon-all" pipeline (http://surfer.nmr.mgh.harvard.edu) (Fischl, 2012), which includes normalization of signal intensity, skull stripping, and automated segmentation and parcellation based on the Desikan-Killiany atlas (Desikan et al., 2006). We further segmented the striatum into its subregions, including the globus pallidum (GP), caudate nucleus (CD), and putamen (PM), to fully study their complex structural connectivity with the VTA and SN by taking advantage of the 7.0 Tesla technology. The main PFC subregions, NAcc, HIP, AMY, GP, CD, and PM were extracted from the FreeSurfer processed T1-weighted images. Based on previous studies, we divided the PFC into six subregions: (1) the superior frontal gyrus (SFG); (2) the rostral and caudal middle frontal gyrus (MFG); (3) the inferior frontal gyrus (IFG), which contained the pars opercularis, pars orbitalis, and pars triangularis; (4) the

medial and lateral orbitofrontal cortex (OFC); (5) the frontal pole (FP); and (6) the rostral and caudal anterior cingulate cortex (ACC). The anterior limb of the internal capsule (ALIC) was extracted from the JHU ICBM-DTI-81 white-matter labels (Oishi et al., 2008) and registered to individual structural images using MRtrix. All the regions of interest (ROIs) are shown in Fig. 2.

Due to the small volume and lack of clear anatomical borders of the VTA, and the high iron content in the SN, segmentation of these two regions posed challenges (Bazin et al., 2020; Forstmann et al., 2017; Johansen-Berg, 2013; Trutti et al., 2019). Therefore, for these two structures that have rarely been considered in MRI atlases and segmentation methods before, we employed Nighres (Huntenburg et al., 2018), a neuroimage analysis package designed for high-resolution neuroimaging, for segmentation. In brief, we utilized an innovative automated segmentation technique, developed based on a large quantitative 7T MRI database, to calculate the R1-maps, R2*-maps, T1-maps, T1-weighted images, T2*-maps, and quantitative susceptibility mapping (QSM) from the MP2RAGEME (Alkemade et al., 2020). This approach facilitated the precise identification and labeling of subcortical structures. This algorithm, which incorporates elements such as shape priors, intensity distribution models, spatial relationships, and global constraints, is named Multi-contrast Anatomical Subcortical Structure Parcellation (MASSP) (Bazin et al., 2020). In order to reduce the omission of streamline capture, we extended the mask of all ROIs outward by one voxel.

2.5. Diffusion data preprocessing

Diffusion data were processed with MRtrix version 3.0.4 and FSL version 6.0.5.2. Briefly, the diffusion images were subjected to denoising, Gibbs ringing removal (Cordero-Grande et al., 2019; Kellner et al., 2016; Veraart et al., 2016a, 2016b), correcting susceptibility-induced distortions, eddy currents, motion artifacts (Andersson et al., 2003; Andersson and Sotiropoulos, 2016; Smith et al., 2004), and inhomogeneity correction (Tustison et al., 2010). Afterward, the corrected diffusion-weighted images were co-registered to T1w space (Jenkinson et al., 2002; Jenkinson and Smith, 2001). A segmented tissue image and a mask image for seeding streamlines at the gray matter-white matter interface were created (Smith et al., 2012). The estimation of the diffusion tensor (Basser et al., 1994; Veraart et al., 2013), the response function for spherical deconvolution (Tournier et al., 2019), and fiber orientation distributions (FOD) (Jeurissen et al., 2014) were performed.

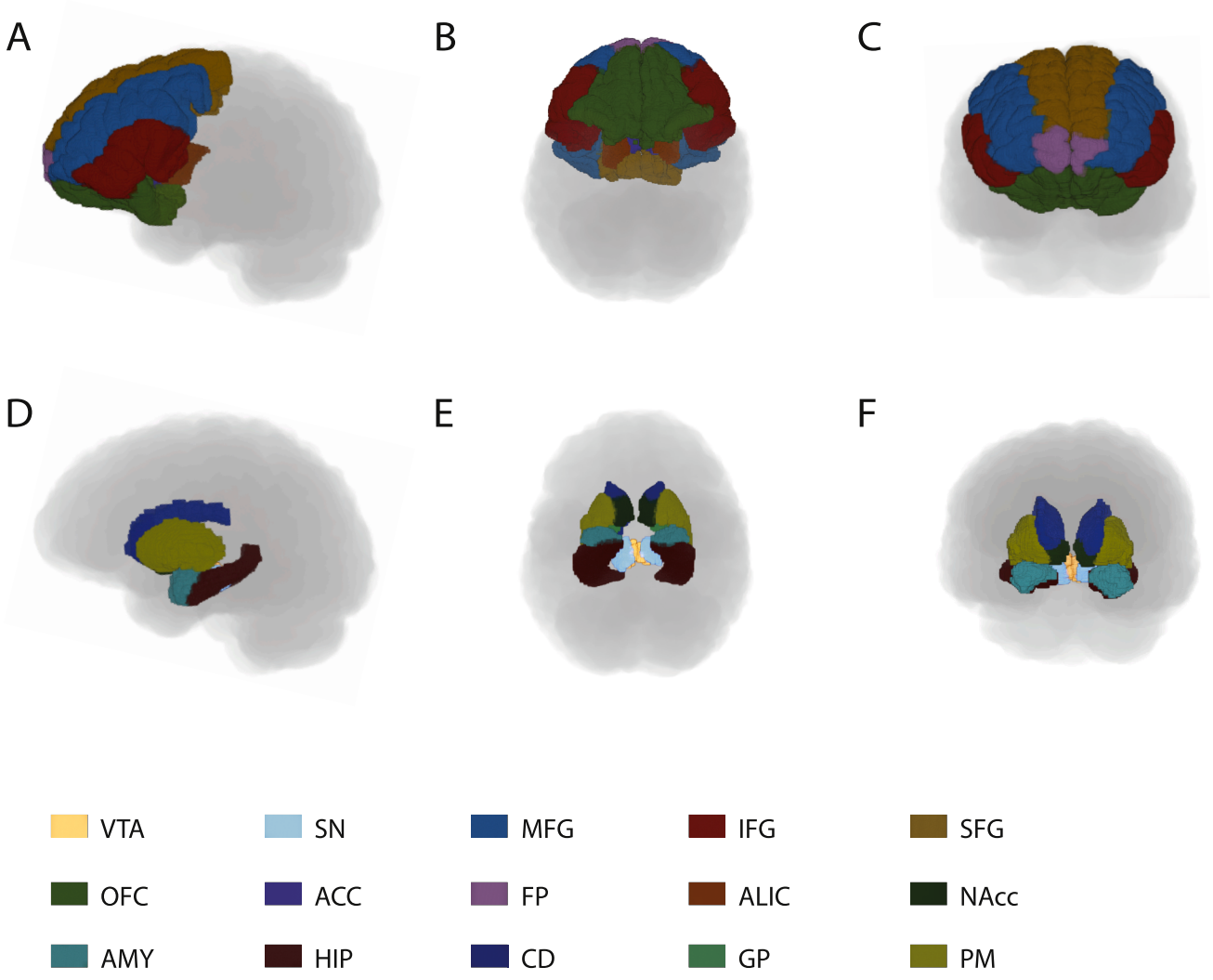

Fig. 2. All the regions of interest.
Figures are arranged in the order of sagittal, axial, and coronal views. Abbreviations: VTA = ventral tegmental area; SN = substantia nigra; MFG = rostral and caudal middle frontal gyrus; IFG = inferior frontal gyrus; SFG = superior frontal gyrus; OFC = medial and lateral orbitofrontal cortex; ACC = rostral and caudal anterior cingulate cortex; FP = frontal pole; ALIC = anterior limb of the internal capsule; NAcc = nucleus accumbens; AMY = amygdala; HIP = hippocampus; CD = caudate nucleus; GP = globus pallidus; PM = putamen.

Finally, we locally fitted the diffusion tensor in each voxel, resulting in whole-brain maps encompassing FA, axial diffusivity (AD), mean diffusivity (MD), and radial diffusivity (RD). Schematic representation of key DTI indices and their properties are shown in Fig. 3 (Heij et al., 2019).

2.6. Tractography

Probabilistic tractography was carried out with MRtrix (Smith et al., 2012; Tournier et al., 2010). The VTA and SN masks were employed as seed regions, initiating 200,000 random seeds. Streamline generation is restricted to the ipsilateral hemisphere of each seed point. Based on the hypothesis, we aimed to obtain the following 15 pairs of tracts: (a) the mesocortical pathway: VTA-SFG, VTA-MFG, VTA-IFG, VTA-OFC, VTA-FP, and VTA-ACC; (b) the mesolimbic pathway: VTA-NAcc, VTA--HIP, and VTA-AMY; (c) the nigrostriatal pathway: SN-CD and SN-PM; (d) considering the DA pathways are more complex than conventionally described (Handfield-Jones, 2019), we also tried to reconstruct the unconventional DA pathways: VTA-GP, VTA-CD, VTA-PM, and SN-GP (Kwon and Jang, 2014). To improve the specificity of the tracking results, we used waypoints and exclusion regions. For the VTA-PFC tracts, the ALIC was used as the waypoint, in line with previous studies (Hosp et al., 2019; King et al., 2022). To achieve more precise white matter fiber pathways, in the case of the VTA-PFC tracts, the cortical areas other than the target cortex were used as exclusion areas. For the VTA-NAcc, VTA-HIP, and VTA-AMY tracts, when the endpoint was NAcc, HIP, or AMY, the other two regions and the whole cortex served as exclusion areas. Similarly, for the VTA-striatum tracts and SN-striatum tracts, when the endpoint was GP, CD, or PM, the other two regions and the whole cortex were designated as exclusion areas. For controlling streamline generation, we established a FOD magnitude cutoff at 0.01 and constrained the maximum angle between successive streamline generation steps to 60°. Microstructural measurements including FA, MD, RD, and AD of each tract were extracted. For enhanced accuracy concerning the ground truth of the white matter and the removal of spurious streamlines, the process of extracting streamline count (SC) integrates spherical deconvolution (SIFT2) weights (Smith et al., 2015).

2.7. Statistical analysis

We conducted our statistical analyses using Bayesian statistics as implemented in JASP (version 0.17.1: https://jasp-stats.org/) (van Doorn et al., 2021). An important advantage of Bayesian Statistics is that it can provide evidence for the alternative as well as the null hypothesis. Moreover, Bayesian Statistics render multiple comparisons correction redundant, as the posterior distribution does not change when additional comparisons are made (Kruschke, 2010). The Bayesian factor (BF) was interpreted using the following evidence categories: $BF < 3$ (and its reciprocal) indicates anecdotal evidence for Hypothesis 1; $BF \geq 3$ corresponds to moderate evidence; $BF \geq 10$ suggests strong evidence; $BF \geq 30$ represents very strong evidence; and $BF \geq 100$ indicates extreme evidence (Lee and Wagenmakers, 2014). Only results with $BF \geq 3$ are reported and discussed.

For basic demographic and clinical data comparisons, the Bayesian chi-square test was used for dichotomous variables, and the Bayesian independent samples t-test for continuous variables. A Bayesian analysis of covariance (ANCOVA) was performed on every white matter metric, including group (MDD/HC) or subgroups (medicated/unmedicated MDD; recurrent episodes/first episode MDD; typical/atypical MDD) as a fixed factor and age, gender, and intracranial volume (ICV) as covariates. The Bayesian ANCOVA works by comparing four models with varying predictors of final course grade: (1) a null model; (2) a model containing only the group as a predictor; (3) models containing only one covariate; (4) several models containing interaction between fixed factor and covariates as predictors. Then we obtained the BF_M, which indicated the change in model odds after observing the data. To account for model uncertainty, we then performed Bayesian model averaging to test the effect of the predictors to obtain BF_{incl}, a primary measure of the strength of evidence for differences between groups.

Finally, Bayesian linear regression analysis was performed to examine if the severity of depression, anxiety symptoms, insomnia, childhood trauma, and age of onset were associated with DA system white matter characteristics among MDD patients. Age, gender, and ICV were again used as covariates, with white matter variables as dependent variables. For highly skewed clinical data, we applied a square root transformation to normalize the data. In the Bayesian linear regression model, we applied a uniform prior to the models, such that all models were set to be equally likely a priori before observing any data, and we applied JZS prior (r scale = 0.354) to the regression coefficients. Results were only retained if there was at least moderate evidence ($BF \geq 3$) after the removal of outliers.

3. Results

3.1. Demographical and clinical variables

A total of 53 MDD patients and 12 HCs were enrolled in the present study. The MDD group comprised 40 females (75.47%), while the HC group included 7 females (58.33%). Among the MDD patients, 22 individuals had recurrent depression (41.51%), with a mean age of onset of 21.33 ± 10.50 years. The Bayesian independent samples t-test and the Bayesian chi-square test provided no evidence that age, gender, and scores of CTQ were different between groups (all $BF_{10} < 3$). Moderate or greater evidence was found suggesting that MDD patients had higher scores of IDS, BAI, and IRS (all $BF_{10} > 3$). Demographical and clinical details are shown in Table 1.

3.2. Reconstruction of DA pathways

To ensure the accuracy of fiber tracking, we inspected each bundle of each participant. As we could not trace VTA-FP and VTA-ACC tracts in over 1/3 of the subjects and did not obtain good-quality VTA-HIP and VTA-AMY tracts, these four tracts were excluded from further analysis. Due to the advantage of ultra-high field and the exclusion of interfering brain regions during reconstruction, the accuracy of our fiber tract imaging is consistent with the results of previous literature (Bracht et al., 2014; Hosp et al., 2019, 2019; Kwon and Jang, 2014; MacNiven et al., 2020; Murray et al., 2023; Plantinga et al., 2016). Fig. 4 and Supplemental Figure 1 show a visualization of all tracts included in the current analysis. Additionally, Supplemental Table 1-5 provides detailed quantitative information on white matter indicators for all tracts, and Table 2 summarizes all BF values of all tracts with moderate or higher evidence.

3.3. Differences in DA pathway connectivity between MDD patients and HCs

The Bayesian ANCOVA showed moderate evidence for lower SC of left SN-PM tracts (belongs to the nigrostriatal pathway) in MDD versus HC participants. The group (MDD/HC) model had its model odds increased after observing data ($BF_M = 7.147$). The data were 6.605 times more likely under models containing group as a predictor ($BF_{incl} = 6.605$, Supplemental Table 6, Fig. 5. A). The Bayesian ANCOVA moreover provided moderate evidence for lower SC of right SN-GP tracts in MDD versus HC participants. The group (MDD/HC) model had its model odds increased after observing data ($BF_M = 6.633$). Moreover, the data were 5.118 times more likely under models containing group as a predictor ($BF_{incl} = 5.118$, Supplemental Table 7, Fig. 5. B). The results did not show conclusive evidence for group differences in the mesolimbic and mesocortical pathways (BF_{incl} range from 0.310 to 1.684).

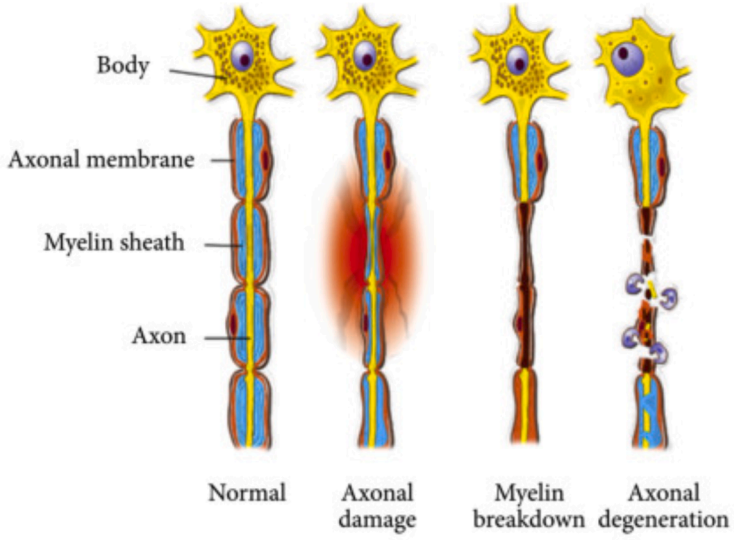

(A)

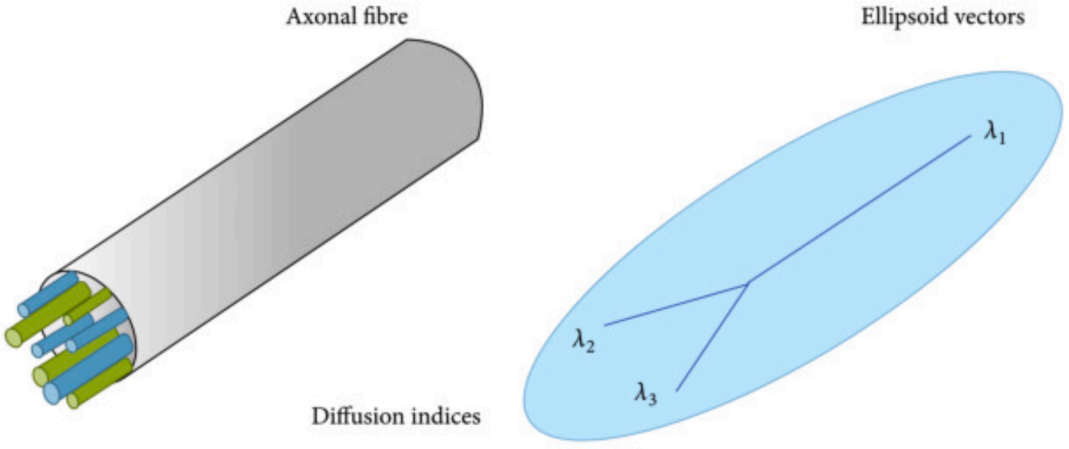

$$FA = \sqrt{\frac{1}{2}} \cdot \frac{\sqrt{(\lambda_1 - \lambda_2)^2 + (\lambda_2 - \lambda_3)^2 + (\lambda_3 - \lambda_1)^2}}{\sqrt{(\lambda_1)^2 + (\lambda_2)^2 + (\lambda_3)^2}} \quad M.Dif = \left(\frac{\lambda_1 + \lambda_2 + \lambda_3}{3}\right) \quad R.Dif = \left(\frac{\lambda_2 + \lambda_3}{2}\right) \quad A.Dif = (\lambda_1)$$

(B)

DTI Index				
Characteristic	**FA**	**A.Dif**	**R.Dif**	**M.Dif**
Diffusivity	In one direction as opposed to all other directions	Along the principal direction of the fiber	Perpendicular to the principal direction of the fiber	Average water diffusion in all directions within the fiber
Tissue Proxy	General WM integrity	Axonal integrity	Myelination level	Cellularity level

(C)

Fig. 3. Schematic representation of key DTI indices and their properties.
Reprinted with permission from Hindawi Publishing Corporation: BioMed Research International (Alves et al., 2015), and Elsevier Publishing: Progress in Neuro-Psychopharmacology and Biological Psychiatry, (Heij et al., 2019).

Table 1
Demographical and clinical information of the participants.

	MDD (n = 53)	HC (n = 12)	BF_{10}
Age (years), mean ± SD	36.57 ± 10.71	34.37 ± 9.67	0.368
Gender (female), n (%)	40 (75.47%)	7 (58.33%)	0.703
Age of onset (years) [a], mean ± SD	21.33 ± 10.50	-	-
Recurrent depression, n (%)	22 (41.51%)	-	-
With atypical MDD [a], n (%)	14 (26.92%)	-	-
IDS [a], mean ± SD	34.21 ± 13.19	4.08 ± 2.81	**7.016E7**
CTQ [a], mean ± SD	47.15 ± 17.78	35.58 ± 6.78	2.082
BAI [a], mean ± SD	14.33 ± 9.67	2.42 ± 2.35	**420.291**
IRS [a], mean ± SD	9.81 ± 5.16	5.25 ± 4.43	**6.851**
With any psychtropic medications, n (%)	30 (56.60%)	-	-
With any antidepressants, n (%)	27 (50.94%)	-	-
With SSRIs and/or SNRIs, n (%)	20 (37.74%)	-	-
With TCA, n (%)	8 (15.09%)	-	-
With atypical antidepressants, n (%)	2 (3.77%)	-	-
With lithium stabilizer, n (%)	3 (5.66%)	-	-
With antipsychotics, n (%)	6 (11.32%)	-	-
With benzodiaz, n (%)	6 (11.32%)	-	-

Bold indicates moderate or greater evidence.
Abbreviation: MDD = major depressive disorder; HC = healthy control; SD = standard deviation; IDS = Inventory for Depressive Symptomatology; CTQ = Childhood Trauma Questionnaire; BAI = Becks Anxiety Inventory; IRS = Insomnia Rating Scale; SSRI = selective serotonin reuptake inhibitor; SNRI = serotonin-norepinephrine reuptake inhibitor; TCA = tricyclic antidepressant.
[a]: One MDD patient did not provide the age of onset, and another MDD patient did not provide data for IDS, IRS, and CTQ. Therefore, when analyzing the data related to these indicators, the sample size for MDD is 52 individuals.

3.4. DA pathway connectivity relates to MDD severity and insomnia features

Although there were no group differences and SC of left VTA-GP was within the normal range (Supplemental Figure 2), strong evidence showed that higher MDD symptom severity (IDS) related to diminished SC of left VTA-GP tracts (BF_{incl} = 13.705, Supplemental Table 8, Fig. 5. C). There was also moderate evidence supporting that higher insomnia severity (IRS) related to elevated RD of left VTA-MFG tracts (BF_{incl} = 5.014, Supplemental Table 9, Fig. 5. D), as well as lower FA of right VTA-SFG tracts (BF_{incl} = 4.579, Supplemental Table 10, Fig. 5. E).

3.5. DA pathway connectivity relates to MDD age of onset

Moderate to strong evidence was also provided that earlier age of MDD onset relates to higher FA of the left SN-GP tracts (BF_{incl} = 12.113, Supplemental Table 11, Fig. 5. F), along with higher FA of the left VTA-SFG tracts (BF_{incl} = 5.245, Supplemental Table 12, Fig. 5. G). Moderate evidence was also found for earlier age of onset relating to lower AD values within three tracts: the left VTA-OFC tracts (BF_{incl} = 6.811, Supplemental Table 13, Fig. 5. H), left VTA-MFG tracts (BF_{incl} = 5.424, Supplemental Table 14, Fig. 5. I), and left VTA-IFG tracts (BF_{incl} = 4.229, Supplemental Table 15, Fig. 5. J).

Moreover, moderate to extreme evidence was found for earlier age of onset relating to lower MD values within six tracts: left VTA-OFC tracts (BF_{incl} = 110.092, Supplemental Table 16, Fig. 5. K), left VTA-MFG tracts (BF_{incl} = 90.007, Supplemental Table 17, Fig. 5. L), left VTA-IFG tracts (BF_{incl} = 54.493, Supplemental Table 18, Fig. 5. M), and left VTA-SFG tracts (BF_{incl} = 43.332, Supplemental Table 19, Fig. 5. N), left VTA-GP tracts (BF_{incl} = 4.440, Supplemental Table 20, Fig. 5. O) right VTA-IFG tracts (BF_{incl} = 3.076, Supplemental Table 21, Fig. 5. P).

Finally, moderate to extreme strong evidence was also found for earlier age of onset relating to lower RD values within eight tracts: left VTA-OFC tracts (BF_{incl} = 402.065, Supplemental Table 22, Fig. 5. Q), left VTA-SFG tracts (BF_{incl} = 281.137, Supplemental Table 23, Fig. 5. R), left VTA-MFG tracts (BF_{incl} = 35.824, Supplemental Table 24, Fig. 5. S), left VTA-IFG tracts (BF_{incl} = 31.275, Supplemental Table 25, Fig. 5. T), left SN-GP tracts (BF_{incl} = 26.247, Supplemental Table 26, Fig. 5. U), left VTA-GP tracts (BF_{incl} = 15.059, Supplemental Table 27, Fig. 5. V), right VTA-SFG tracts (BF_{incl} = 10.039, Supplemental Table 28, Fig. 5. W), and right VTA-IFG tracts (BF_{incl} = 4.720, Supplemental Table 29, Fig. 5. X).

In addition, no evidence was found for the association between white matter metrics of DA pathways and medication status, recurrence, typical type, and scores of BAI and CTQ (all $BF_{incl} < 3$).

4. Discussion

This study represents the first investigation of the structural connectivity architecture of major DA pathways in MDD using UHF dMRI at 7.0 Tesla. Previous research on white matter connectivity of DA pathways has almost exclusively employed standard field strength MRI (1.5/3.0 Tesla), and primarily focused on the mesocortical DA pathway. By means of UHF MRI and advanced segmentation of subcortical structures, we conducted fiber tracking of DA pathways, with refining the segmentation of the VTA/SN-striatum tracts. Through this approach, we uncovered novel white matter connectivity changes previously overlooked in the literature and identified white matter tracts that were previously undisclosed in relation to MDD clinical indicators. Specifically, we found that MDD relates to perturbed nigrostriatal pathway connectivity, while several MDD clinical characteristics (severity of depression/age of onset/insomnia) correspond with changes of connectivity within mesocortical, nigrostriatal, and unconventional DA pathways. These alterations within cortical and subcortical DA circuits may influence sensory processing, emotion regulation, and goal-directed behavior. The findings allow uniquely fine-grained insights into the structural architecture and integrity of several DA pathways in MDD, and cautiously implicate their involvement in the clinical manifestation of MDD.

Our study has found that white matter abnormalities in the DA pathway are significantly associated with MDD. DA is involved in mood regulation, reward mechanisms, and motivation (Hori and Kunugi, 2013). MDD patients often exhibit abnormal DA function (Dunlop and Nemeroff, 2007; Engström et al., 1999; Reddy et al., 1992), resulting in reduced feelings of pleasure and a lack of motivation. White matter abnormalities may lead to altered efficiency of information transmission, causing an imbalance in the function of the DA pathway. This imbalance in structural connectivity may further affect the ability of the brain to regulate emotions and process rewards, playing a role in the onset and progression of MDD.

4.1. MDD relates to the nigrostriatal DA pathway

Contrary to previous standard field strength MRI work (1.5/3.0 Tesla) which showed that DA pathway abnormalities in MDD are mostly concentrated in the mesocortical pathway, this UHF dMRI study shows that DA pathway abnormalities in MDD also include shifts in nigrostriatal pathway connectivity. One study reported that MDD patients exhibited lower FA in the right VTA-lateral OFC and VTA-dorsolateral PFC tracts relative to HCs. This finding was restricted to patients with melancholic symptoms (Bracht et al., 2014). Another study suggested a reduction in fiber bundle volume and fiber bundle count in the left superolateral medial forebrain bundle (MFB) of MDD patients, but did not observe differences in the inferomedial MFB (Bracht et al., 2022). Based on the similarities in tract reconstruction, the superolateral MFB relates to our mesocortical pathway, and the inferomedial MFB to our mesolimbic pathway. Differences in results between this and our study could be related to the considerable difference in imaging resolution (10.6 mm^3 prior work versus 2.7 mm^3 our study), and our separation between VTA projections to different cortical regions, while the other

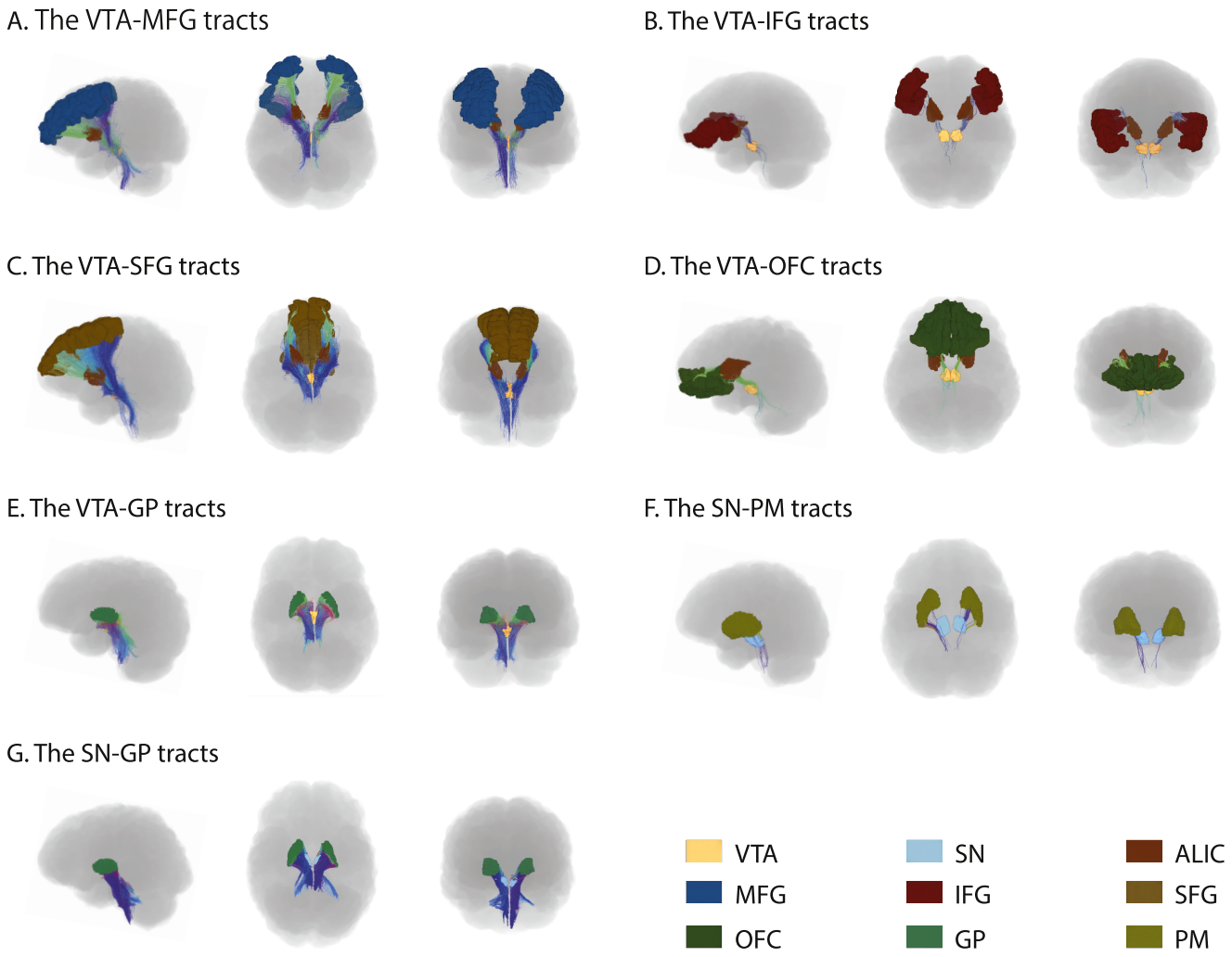

Fig. 4. All tracts with moderate or greater evidence.
Figures are arranged in the order of sagittal, axial, and coronal views. Abbreviation: VTA = ventral tegmental area; SN = substantia nigra; ALIC = anterior limb of the internal capsule; SFG = superior frontal gyrus; MFG = rostral and caudal middle frontal gyrus; IFG = inferior frontal gyrus; OFC = medial and lateral orbitofrontal cortex; GP = globus pallidus; PM = putamen.

study did not distinguish between cortical target projections. So, although the studies cannot be compared directly, our results suggest that we could not replicate the results of differences in meso-cortical/superolateral MFB pathways using more accurate measurements (Coenen et al., 2022).

Instead, we found that MDD patients have lower SC in the nigrostriatal pathway (left SN-PM) and the unconventional DA pathway (SN-GP tracts) compared to HCs. The nigrostriatal pathway has often been reported in the studies of Parkinson's disease and schizophrenia (Kalia and Lang, 2015; Rivas-Grajales et al., 2019). Prior evidence suggests that MDD patients are at a higher risk of developing Parkinson's disease (Schapira et al., 2017), and patients with Parkinson's disease and schizophrenia often exhibit comorbid depressive symptoms (Bloem et al., 2021; Mueser and McGurk, 2004). Similar to MDD, both of these conditions are closely linked to DA dysfunction and anhedonia (Assogna et al., 2011; Lambert et al., 2018; Mhyre et al., 2012). It is generally believed that dysfunction of the DA system in the nigrostriatal pathway is specifically related to motor deficits (Trutti et al., 2019), but a study has also indicated its involvement with the reward system (Wise, 2009), prompting a reconsideration of its role in depression. High-frequency stimulation of the SN can induce anhedonia and decreased motivation in animal models (Tan et al., 2013). Furthermore, an animal study indicated that the nigrostriatal pathway may contribute to the pathogenesis of depression, with dopamine transporter function possibly playing a pivotal role in this regard (Jia and Pittman, 2014). While there is potential evidence indicating the involvement of the nigrostriatal pathway in MDD, the white matter features related to its role in the pathophysiology of human MDD have been unveiled through this only UHF dMRI study to date.

The dorsal striatum is also a part of the nigrostriatal pathway (Fig. 1). It is not only associated with cognitive processes and motivation, but also involved in emotion regulation (Koolschijn et al., 2009). Greater connectivity of the striatum within the reward network is linked to an increased likelihood of depressive disorders (Pan et al., 2022). Furthermore, elevated node strength in the left striatum seems indicative of an elevated risk of developing depressive disorder in the future (Pan et al., 2017). MDD patients show diminished striatal responses both in reward anticipation and reward outcome (Forbes et al., 2009). The PM, as part of the striatum, has also been closely linked with MDD pathophysiology. MDD patients who had attempted suicide exhibited a lower voxel count of gray matter in the PM compared to HCs (Dombrovski et al., 2012). The bilateral PM exhibited significant volume reductions in MDD patients compared to HCs (Lu et al., 2016). Regarding the GP, MDD patients display decreased volume asymmetry when compared to HCs, and the volume of the left GP is positively correlated with the number of previous depressive episodes (Lacerda

Table 2
Summary of the BF values of white matter tracts with moderate or higher evidence for group differences and relationship with clinical indicators.

	BF_{incl}
The Bayesain ANCOVA analysis	
MDD versus HC	
SC of left SN-PM tracts	6.605
SC of right SN-GP tracts	5.118
The Bayesain linear regression analysis	
IDS	
SC of left VTA-GP tracts	13.705
IRS	
RD of left VTA-MFG tracts	5.014
FA of right VTA-SFG tracts	4.579
Age of onset	
RD of left VTA-OFC tracts	402.065
RD of left VTA-SFG tracts	281.137
MD of left VTA-OFC tracts	110.092
MD of left VTA-MFG tracts	90.007
MD of left VTA-IFG tracts	54.493
MD of left VTA-SFG tracts	43.332
RD of left VTA-MFG tracts	35.824
RD of left VTA-IFG tracts	31.275
RD of left SN-GP tracts	26.247
RD of left VTA-GP tracts	15.059
FA of left SN-GP tracts	12.113
RD of right VTA-SFG tracts	10.039
AD of left VTA-OFC tracts	6.811
AD of left VTA-MFG tracts	5.424
FA of left VTA-SFG tracts	5.245
RD of right VTA-IFG tracts	4.720
MD of left VTA-GP tracts	4.440
AD of left VTA-IFG tracts	4.229
MD of right VTA-IFG tracts	3.076

Abbreviation: MDD = major depressive disorder; HC = healthy control; FA = fractional anisotropy; AD = axial diffusivity; MD = mean diffusivity; RD = radial diffusivity; SC = streamline count; VTA = ventral tegmental area; MFG = rostral and caudal middle frontal gyrus; IFG = inferior frontal gyrus; SFG = superior frontal gyrus; OFC = medial and lateral orbitofrontal cortex; GP = globus pallidus; PM = putamen; SN = substantia nigra.

et al., 2003). The severity of suicidal risk in MDD patients with suicidal ideation is positively correlated with the level of atrophy in the left GP (Kim et al., 2019). Additionally, there have been reported cases of acute depressive symptoms in Parkinson's patients following DBS stimulation of the GP (Philipsson et al., 2017).

4.2. MDD severity and insomnia relate to unconventional and mesocortical DA pathways

In the present study, the severity of depression was negatively associated with SC of the VTA-GP pathway, and insomnia was positively associated with loss of white matter integrity in the mesocortical pathway. VTA is one of the primary sources of DA in the brain and is associated with changes in anhedonia, motivation, and reward learning/prediction (Markovic et al., 2021; Trutti et al., 2019). The significant role of the GP in MDD has already been discussed above. These pieces of evidence support the previously neglected correlation that our study revealed between VTA-GP tracts and the severity of depressive symptoms. Moreover, prior findings also suggested a correlation between insomnia and diminished white matter integrity (Sexton et al., 2019). Sleep loss is associated with dysfunction of the DA system (López-Muciño et al., 2022). Furthermore, sleep disturbances are common in both patients with Parkinson's disease and those with schizophrenia, both of which are primarily involved in DA imbalance (Bloem et al., 2021; Ferrarelli, 2021). Our study findings suggest that white matter alterations in the mesocortical pathway are involved in insomnia associated with MDD.

4.3. MDD age of onset relates to most of the DA pathways

Interestingly, we found that white matter integrity of mesocortical, nigrostriatal, and unconventional DA pathways was associated with MDD age of onset, wherein the mesocortical pathway seemed most heavily affected. The mesocortical pathway projects from the VTA to the PFC (Fig. 1). A study using 7.0 Tesla magnetization transfer (MT) MRI found that patients with depression and anxiety disorders have reduced structural integrity in the dopaminergic VTA compared to HCs (Morris et al., 2022). However, in our study, the white matter of the mesocortical pathway appears not to play a significant role in between-group differences but rather in the within-group correlations with clinical indicators in MDD. Furthermore, among white matter indices with moderate or stronger evidence, all of the FA measures are negatively correlated with the age of onset. This seems to suggest that a later onset of MDD may be associated with more severe general white matter damage in the DA pathways. Our study participants had an average age of onset of 21.33 ± 10.50 years (with a median age of onset at 18 years), indicating that half of them experienced depression before reaching adulthood.

Brain development is indeed heterochronous, meaning that distinct structures and functions of brain regions and circuits mature at different rates (Giedd et al., 1999; Steinberg, 2005). During adolescence, a significant amount of myelin sheath (a crucial component of brain white matter) forms in the brain, strengthening tracts within the prefrontal cortex (the endpoint of the mesocortical pathway) and throughout the entire brain (Baez and Heller, 2020). In the later stages of adolescence, there is a reduction in surplus tracts, leading to the formation of more efficient neural circuits (Steinberg, 2005). Therefore, the brain undergoes significant neural remodelling throughout development before it reaches full maturity. We speculate that the white matter in the DA system may retain strong neural plasticity even after suffering damage from the illness at a younger age, while individuals who develop the illness after brain maturity may experience more significant damage due to a reduced capacity for brain repair. Looking at it from another perspective, it is also possible that the onset of MDD is caused by white matter degeneration over time, either due to physiological or pathological reasons. Future research could focus on exploring the association between the longitudinal development of MDD and white matter changes in the DA system, providing a deeper understanding of whether white matter abnormalities in the DA pathways change with the progression of MDD.

Last but not least, it is important to mention that the brain regions we investigated in our study, related to several DA pathways, not only contain DA-producing neurons but also a smaller portion of serotonin-, GABA-, and glutamate-producing neurons (Morales and Margolis, 2017). Therefore, it is important to exercise caution when directly associating our research findings solely with DA.

5. Limitations

This study has several limitations. Due to cost and time constraints when conducting UHF MRI research, we chose to maximize and prioritize the inclusion of our main target group (MDD), which resulted in a relatively small HC sample. This could potentially limit the power to detect subtle differences between MDD and HC or perhaps inflate some effects (Type I & Type II errors). Future UHF MRI work on the topic is warranted in larger and more balanced samples, to further explore and validate our findings. That said, the 53 MDD patients included here render this the largest UHF MRI examination of the brain in MDD to date. This is also a cross-sectional study, which does not allow us to establish whether the white matter abnormalities in DA pathways are a cause or a consequence of MDD. Due to the unavailability of precise fiber bundle imaging for VTA-HIP and VTA-AMY tracts, they were excluded from the analysis. Nevertheless, the remaining streamlines were accurately reconstructed, enabling an unprecedentedly extensive and in-depth exploration of DA pathways in MDD patients. Finally, we did

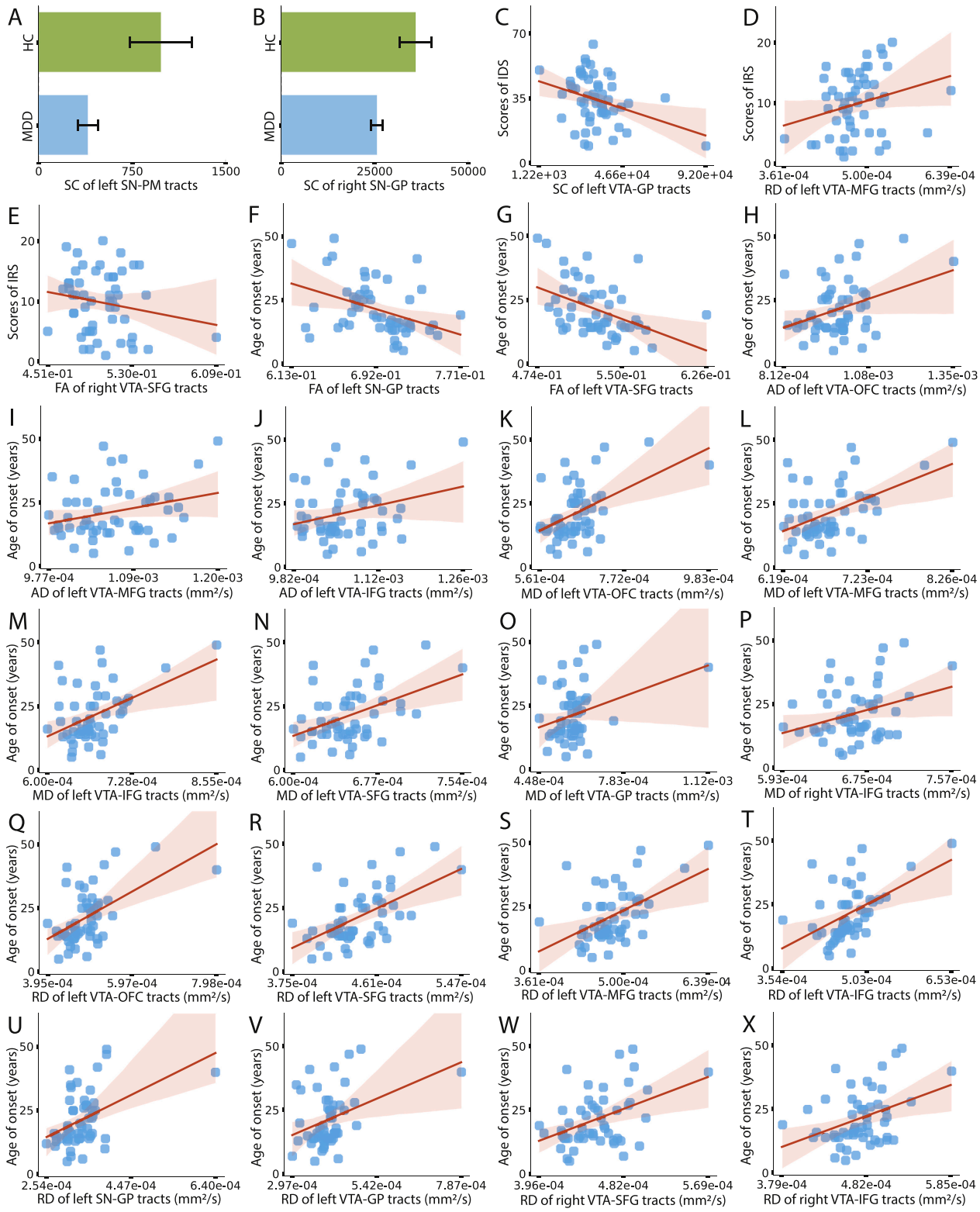

Fig. 5. Differences in white matter characteristics of the DA pathways between MDD and HC and their relationship with clinical indices in MDD.
Abbreviations: DA = dopamine; MDD = major depressive disorder; HC = healthy control; FA = fractional anisotropy; AD = axial diffusivity; MD = mean diffusivity; RD = radial diffusivity; SC = streamline count; VTA = ventral tegmental area; SN = substantia nigra; SFG = superior frontal gyrus; MFG = rostral and caudal middle frontal gyrus; IFG = inferior frontal gyrus; OFC = medial and lateral orbitofrontal cortex; GP = globus pallidus; PM = putamen.

not have a scale specifically for anhedonia, so we could not map DA-anhedonia relations in our MDD patients.

6. Conclusions

In summary, we identify novel white matter alterations within several DA pathways amongst MDD patients that were overlooked by

previous studies. These alterations within cortical and subcortical DA circuits might influence sensory processing, emotion regulation, and goal-directed behavior in MDD patients. These findings fill critical knowledge gaps, by allowing uniquely fine-grained insights into structural architecture and integrity of several DA pathways that may underpin the clinical manifestation of MDD. Future work should examine how MDD progression and treatment response map onto DA pathway architecture and associated network-level function.

Contributor

Weijian Liu: data analysis, manuscript writing, manuscript revision; **Jurjen Heij:** data analysis, manuscript revision; **Shu Liu:** data analysis, manuscript revision; **Luka Liebrand:** manuscript revision; **Matthan Caan:** study design, manuscript revision; **Wietske van der Zwaag:** study design, manuscript revision; **Dick J Veltman:** study design, manuscript revision; **Lin Lu:** manuscript revision; **Moji Aghajani:** study design, manuscript revision; **Guido van Wingen:** study design, manuscript revision.

Role of funding source

This research was funded by Amsterdam Neuroscience (Alliance Project Grant to M. Aghajani and G.A. van Wingen) and the Department of Psychiatry, Amsterdam UMC, Location VUmc. Weijian Liu was supported by the China Scholarship Council.

Declaration of competing interest

Matthan Caan is a shareholder of Nico-lab International Ltd. Guido van Wingen has received research support from Philips for unrelated work. The other authors declare that they have no conflict of interest.

Data availability statement

Data will be available from the corresponding author upon reasonable request.

Acknowledgment

The authors are extremely grateful to all participants involved in the study and gratefully acknowledge the contributions of SPINOZA Center for Neuroimaging Amsterdam and GGZ InGeest Amsterdam.

Supplementary materials

Supplementary material associated with this article can be found, in the online version, at doi:10.1016/j.euroneuro.2024.07.014.

References

Alkemade, A., Mulder, M.J., Groot, J.M., Isaacs, B.R., Van Berendonk, N., Lute, N., Isherwood, S.J., Bazin, P.-L., Forstmann, B.U., 2020. The Amsterdam Ultra-high field adult lifespan database (AHEAD): a freely available multimodal 7 Tesla submillimeter magnetic resonance imaging database. NeuroImage 221, 117200. https://doi.org/10.1016/j.neuroimage.2020.117200.

Andersson, J.L.R., Skare, S., Ashburner, J., 2003. How to correct susceptibility distortions in spin-echo echo-planar images: application to diffusion tensor imaging. NeuroImage 20, 870–888. https://doi.org/10.1016/S1053-8119(03)00336-7.

Andersson, J.L.R., Sotiropoulos, S.N., 2016. An integrated approach to correction for off-resonance effects and subject movement in diffusion MR imaging. NeuroImage 125, 1063–1078. https://doi.org/10.1016/j.neuroimage.2015.10.019.

Assogna, F., Cravello, L., Caltagirone, C., Spalletta, G., 2011. Anhedonia in Parkinson's disease: a systematic review of the literature. Mov. Disord. Off. J. Mov. Disord. Soc. 26, 1825–1834. https://doi.org/10.1002/mds.23815.

Baez, L.M., Heller, A.S., 2020. Impact of age at onset on the phenomenology of depression in treatment-seeking adults in the STAR*D trial. J. Affect. Disord. 262, 381–388. https://doi.org/10.1016/j.jad.2019.10.036.

Basser, P.J., Mattiello, J., LeBihan, D., 1994. Estimation of the effective self-diffusion tensor from the NMR spin echo. J. Magn. Reson. B 103, 247–254. https://doi.org/10.1006/jmrb.1994.1037.

Bazin, P.-L., Alkemade, A., Mulder, M.J., Henry, A.G., Forstmann, B.U., 2020. Multi-contrast anatomical subcortical structures parcellation. eLife 9, e59430. https://doi.org/10.7554/eLife.59430.

Beck, A.T., Epstein, N., Brown, G., Steer, R.A., 1988. An inventory for measuring clinical anxiety: psychometric properties. J. Consult. Clin. Psychol. 56, 893.

Belmaker, R.H., 2008. Major depressive disorder. N. Engl. J. Med. 14.

Belujon, P., Grace, A.A., 2017. Dopamine system dysregulation in major depressive disorders. Int. J. Neuropsychopharmacol. 20, 1036–1046. https://doi.org/10.1093/ijnp/pyx056.

Bloem, B.R., Okun, M.S., Klein, C., 2021. Parkinson's disease. Lancet Lond. Engl. 397, 2284–2303. https://doi.org/10.1016/S0140-6736(21)00218-X.

Bosker, F.J., Tanke, M.A.C., Jongsma, M.E., Cremers, T.I.F.H., Jagtman, E., Pietersen, C. Y., van der Hart, M.G.C., Gladkevich, A.V., Kema, I.P., Westerink, B.H.C., Korf, J., den Boer, J.A., 2010. Biochemical and behavioral effects of long-term citalopram administration and discontinuation in rats: Role of serotonin synthesis. Neurochem. Int. 57, 948–957. https://doi.org/10.1016/j.neuint.2010.10.001.

Bracht, T., Horn, H., Strik, W., Federspiel, A., Schnell, S., Höfle, O., Stegmayer, K., Wiest, R., Dierks, T., Müller, T.J., Walther, S., 2014. White matter microstructure alterations of the medial forebrain bundle in melancholic depression. J. Affect. Disord. 155, 186–193. https://doi.org/10.1016/j.jad.2013.10.048.

Bracht, T., Mertse, N., Walther, S., Lüdi, K., Breit, S., Federspiel, A., Wiest, R., Denier, N., 2022. Link between structural connectivity of the medial forebrain bundle, functional connectivity of the ventral tegmental area, and anhedonia in unipolar depression. NeuroImage Clin 34, 102961. https://doi.org/10.1016/j.nicl.2022.102961.

Bunney, W.E., Davis, J.M., 1965. Norepinephrine in depressive reactions. A review. Arch. Gen. Psychiatry 13, 483–494. https://doi.org/10.1001/archpsyc.1965.01730060001001.

Caan, M.W.A., Bazin, P.-L., Marques, J.P., de Hollander, G., Dumoulin, S.O., van der Zwaag, W., 2019. MP2RAGEME: T1, T2*, and QSM mapping in one sequence at 7 tesla. Hum. Brain Mapp 40, 1786–1798. https://doi.org/10.1002/hbm.24490.

Coenen, V.A., Döbrössy, M.D., Teo, S.J., Wessolleck, J., Sajonz, B.E.A., Reinacher, P.C., Thierauf-Emberger, A., Spittau, B., Leupold, J., Von Elverfeldt, D., Schlaepfer, T.E., Reisert, M., 2022. Diverging prefrontal cortex fiber connection routes to the subthalamic nucleus and the mesencephalic ventral tegmentum investigated with long range (normative) and short range (ex-vivo high resolution) 7T DTI. Brain Struct. Funct. 227, 23–47. https://doi.org/10.1007/s00429-021-02373-x.

Coppen, A., 1967. The biochemistry of affective disorders. Br. J. Psychiatry J. Ment. Sci. 113, 1237–1264. https://doi.org/10.1192/bjp.113.504.1237.

Cordero-Grande, L., Christiaens, D., Hutter, J., Price, A.N., Hajnal, J.V., 2019. Complex diffusion-weighted image estimation via matrix recovery under general noise models. NeuroImage 200, 391–404. https://doi.org/10.1016/j.neuroimage.2019.06.039.

de Graaf, R., Bijl, R.V., Smit, F., Vollebergh, W.A.M., Spijker, J., 2002. Risk factors for 12-month comorbidity of mood, anxiety, and substance use disorders: findings from the netherlands mental health survey and incidence study. Am. J. Psychiatry 159, 620–629. https://doi.org/10.1176/appi.ajp.159.4.620.

Desikan, R.S., Ségonne, F., Fischl, B., Quinn, B.T., Dickerson, B.C., Blacker, D., Buckner, R.L., Dale, A.M., Maguire, R.P., Hyman, B.T., Albert, M.S., Killiany, R.J., 2006. An automated labeling system for subdividing the human cerebral cortex on MRI scans into gyral based regions of interest. NeuroImage 31, 968–980. https://doi.org/10.1016/j.neuroimage.2006.01.021.

Dombrovski, A.Y., Siegle, G.J., Szanto, K., Clark, L., Reynolds, C.F., Aizenstein, H., 2012. The temptation of suicide: striatal gray matter, discounting of delayed rewards, and suicide attempts in late-life depression. Psychol. Med. 42, 1203–1215. https://doi.org/10.1017/S0033291711002133.

Dunlop, B.W., Nemeroff, C.B., 2007. The role of dopamine in the pathophysiology of depression. Arch. Gen. Psychiatry 64, 327–337. https://doi.org/10.1001/archpsyc.64.3.327.

Engström, G., Alling, C., Blennow, K., Regnéll, G., Träskman-Bendz, L., 1999. Reduced cerebrospinal HVA concentrations and HVA/5-HIAA ratios in suicide attempters. Monoamine metabolites in 120 suicide attempters and 47 controls. Eur. Neuropsychopharmacol. J. Eur. Coll. Neuropsychopharmacol. 9, 399–405. https://doi.org/10.1016/s0924-977x(99)00016-4.

Fava, G.A., 2020. May antidepressant drugs worsen the conditions they are supposed to treat? The clinical foundations of the oppositional model of tolerance. Ther. Adv. Psychopharmacol. 10, 2045125320970325. https://doi.org/10.1177/2045125320970325.

Fava, M., 2003. Diagnosis and definition of treatment-resistant depression. Biol Psychiatry 53, 649–659. https://doi.org/10.1016/s0006-3223(03)00231-2.

Ferrarelli, F., 2021. Sleep abnormalities in schizophrenia: state of the art and next steps. Am. J. Psychiatry. https://doi.org/10.1176/appi.ajp.2020.20070968.

Fischl, B., 2012. FreeSurfer. NeuroImage 62, 774–781. https://doi.org/10.1016/j.neuroimage.2012.01.021.

Forbes, E.E., Hariri, A.R., Martin, S.L., Silk, J.S., Moyles, D.L., Fisher, P.M., Brown, S.M., Ryan, N.D., Birmaher, B., Axelson, D.A., Dahl, R.E., 2009. Altered striatal activation predicting real-world positive affect in adolescent major depressive disorder. Am. J. Psychiatry 166, 64–73. https://doi.org/10.1176/appi.ajp.2008.07081336.

Forstmann, B.U., de Hollander, G., van Maanen, L., Alkemade, A., Keuken, M.C., 2017. Towards a mechanistic understanding of the human subcortex. Nat. Rev. Neurosci. 18, 57–65. https://doi.org/10.1038/nrn.2016.163.

Gangadhar, B.N., Rao, N.P., 2015. *Action of Antipsychotics*, in: Toga, A.W. (Ed.), Brain Mapping. Academic Press, Waltham, pp. 937–941. https://doi.org/10.1016/B978-0-12-397025-1.00115-9.

Giedd, J.N., Blumenthal, J., Jeffries, N.O., Castellanos, F.X., Liu, H., Zijdenbos, A., Paus, T., Evans, A.C., Rapoport, J.L., 1999. Brain development during childhood and adolescence: a longitudinal MRI study. Nat. Neurosci. 2, 861–863. https://doi.org/10.1038/13158.

Handfield-Jones, N., 2019. Connectomic analysis of substantia nigra pars compacta and ventral tegmental area projections to the striatum and cortex. Electron. Thesis Diss. Repos.

Heij, G.J., Penninx, B.W.H.J., van Velzen, L.S., van Tol, M.-J., van der Wee, N.J.A., Veltman, D.J., Aghajani, M., 2019. White matter architecture in major depression with anxious distress symptoms. Prog. Neuropsychopharmacol. Biol. Psychiatry 94, 109664. https://doi.org/10.1016/j.pnpbp.2019.109664.

Heij, G.J., van der Zwaag, W., Caan, M.W.A., van Wingen, G.A., Aghajani, M., 2022. *Measures of Quantitative MRI Relate to Severity of Major Depressive Disorder*. Presented at the ISMRM, London.

Hori, H., Kunugi, H., 2013. Dopamine agonist-responsive depression. Psychogeriatrics 13, 189–195. https://doi.org/10.1111/psyg.12014.

Hosp, J.A., Coenen, V.A., Rijntjes, M., Egger, K., Urbach, H., Weiller, C., Reisert, M., 2019. Ventral tegmental area connections to motor and sensory cortical fields in humans. Brain Struct. Funct. 224, 2839–2855. https://doi.org/10.1007/s00429-019-01939-0.

Huntenburg, J.M., Steele, C.J., Bazin, P.-L., 2018. Nighres: processing tools for high-resolution neuroimaging. GigaScience 7, giy082. https://doi.org/10.1093/gigascience/giy082.

Jauhar, S., Arnone, D., Baldwin, D.S., Bloomfield, M., Browning, M., Cleare, A.J., Corlett, P., Deakin, J.F.W., Erritzoe, D., Fu, C., Fusar-Poli, P., Goodwin, G.M., Hayes, J., Howard, R., Howes, O.D., Juruena, M.F., Lam, R.W., Lawrie, S.M., McAllister-Williams, H., Marwaha, S., Matuskey, D., McCutcheon, R.A., Nutt, D.J., Pariante, C., Pillinger, T., Radhakrishnan, R., Rucker, J., Selvaraj, S., Stokes, P., Upthegrove, R., Yalin, N., Yatham, L., Young, A.H., Zahn, R., Cowen, P.J., 2023. A leaky umbrella has little value: evidence clearly indicates the serotonin system is implicated in depression. Mol. Psychiatry 28, 3149–3152. https://doi.org/10.1038/s41380-023-02095-y.

Jenkinson, M., Bannister, P., Brady, M., Smith, S., 2002. Improved optimization for the robust and accurate linear registration and motion correction of brain images. NeuroImage 17, 825–841. https://doi.org/10.1016/s1053-8119(02)91132-8.

Jenkinson, M., Smith, S., 2001. A global optimisation method for robust affine registration of brain images. Med. Image Anal. 5, 143–156. https://doi.org/10.1016/s1361-8415(01)00036-6.

Jeurissen, B., Tournier, J.-D., Dhollander, T., Connelly, A., Sijbers, J., 2014. Multi-tissue constrained spherical deconvolution for improved analysis of multi-shell diffusion MRI data. NeuroImage 103, 411–426. https://doi.org/10.1016/j.neuroimage.2014.07.061.

Jia, M., Pittman, J., 2014. Deficits in striatal dopamine and hippocampal serotonin following induction of anxiety/depressive-like behaviors by Bisphenol A. Arch. Neurosci. 2. https://doi.org/10.5812/archneurosci.18555.

Johansen-Berg, H., 2013. Human connectomics — What will the future demand? NeuroImage, Mapp. Connectome 80, 541–544. https://doi.org/10.1016/j.neuroimage.2013.05.082.

Kalia, L.V., Lang, A.E., 2015. Parkinson's disease. Lancet Lond. Engl. 386, 896–912. https://doi.org/10.1016/S0140-6736(14)61393-3.

Katz, M.M., Tekell, J.L., Bowden, C.L., Brannan, S., Houston, J.P., Berman, N., Frazer, A., 2004. Onset and early behavioral effects of pharmacologically different antidepressants and placebo in depression. Neuropsychopharmacology 29, 566–579. https://doi.org/10.1038/sj.npp.1300341.

Kellner, E., Dhital, B., Kiselev, V.G., Reisert, M., 2016. Gibbs-ringing artifact removal based on local subvoxel-shifts. Magn. Reson. Med. 76, 1574–1581. https://doi.org/10.1002/mrm.26054.

Kim, K., Shin, J.-H., Myung, W., Fava, M., Mischoulon, D., Papakostas, G.I., Choi, K.W., Na, E.J., Seo, S.W., Seong, J.-K., Jeon, H.J., 2019. Deformities of the Globus pallidus are associated with severity of suicidal ideation and impulsivity in patients with major depressive disorder. Sci. Rep. 9, 7462. https://doi.org/10.1038/s41598-019-43882-4.

King, S.G., Gaudreault, P.-O., Malaker, P., Kim, J., Alia-Klein, N., Xu, J., Goldstein, R.Z., 2022. Prefrontal-habenular microstructural impairments in human cocaine and heroin addiction. Neuron 110, 3820–3832. https://doi.org/10.1016/j.neuron.2022.09.011 e4.

Klein, D.F., 1974. Endogenomorphic depression. A conceptual and terminological revision. Arch. Gen. Psychiatry 31, 447–454. https://doi.org/10.1001/archpsyc.1974.01760160005001.

Klein, M.O., Battagello, D.S., Cardoso, A.R., Hauser, D.N., Bittencourt, J.C., Correa, R.G., 2019. Dopamine: functions, signaling, and association with neurological diseases. Cell. Mol. Neurobiol. 39, 31–59. https://doi.org/10.1007/s10571-018-0632-3.

Koolschijn, P.C.M.P., van Haren, N.E.M., Lensvelt-Mulders, G.J.L.M., Hulshoff Pol, H.E., Kahn, R.S., 2009. Brain volume abnormalities in major depressive disorder: A meta-analysis of magnetic resonance imaging studies. Hum. Brain Mapp. 30, 3719–3735. https://doi.org/10.1002/hbm.20801.

Kruschke, J.K., 2010. What to believe: Bayesian methods for data analysis. Trends Cogn. Sci. 14, 293–300. https://doi.org/10.1016/j.tics.2010.05.001.

Kwon, D.-H., Paek, S.H., Kim, Y.-B., Lee, H., Cho, Z.-H., 2021. In vivo 3D reconstruction of the human pallidothalamic and nigrothalamic pathways with super-resolution 7T MR track density imaging and fiber tractography. Front. Neuroanat. 15.

Kwon, H.G., Jang, S.H., 2014. Differences in neural connectivity between the substantia nigra and ventral tegmental area in the human brain. Front. Hum. Neurosci. 8.

Lacerda, A.L.T., Nicoletti, M.A., Brambilla, P., Sassi, R.B., Mallinger, A.G., Frank, E., Kupfer, D.J., Keshavan, M.S., Soares, J.C., 2003. Anatomical MRI study of basal ganglia in major depressive disorder. Psychiatry Res 124, 129–140. https://doi.org/10.1016/s0925-4927(03)00123-9.

Lambert, C., Da Silva, S., Ceniti, A.K., Rizvi, S.J., Foussias, G., Kennedy, S.H., 2018. Anhedonia in depression and schizophrenia: A transdiagnostic challenge. CNS Neurosci. Ther. 24, 615–623. https://doi.org/10.1111/cns.12854.

Lee, M.D., Wagenmakers, E.-J., 2014. Bayesian Cognitive Modeling: A Practical Course. Cambridge university press.

Levine, D.W., Kaplan, R.M., Kripke, D.F., Bowen, D.J., Naughton, M.J., Shumaker, S.A., 2003. Factor structure and measurement invariance of the Women's Health Initiative Insomnia Rating Scale. Psychol. Assess. 15, 123–136. https://doi.org/10.1037/1040-3590.15.2.123.

Liebrand, L.C., van Wingen, G.A., Vos, F.M., Denys, D., Caan, M.W.A., 2020. Spatial versus angular resolution for tractography-assisted planning of deep brain stimulation. NeuroImage Clin. 25, 102116. https://doi.org/10.1016/j.nicl.2019.102116.

López-Muciño, L.A., García-García, F., Cueto-Escobedo, J., Acosta-Hernández, M., Venebra-Muñoz, A., Rodríguez-Alba, J.C., 2022. Sleep loss and addiction. Neurosci. Biobehav. Rev. 141, 104832. https://doi.org/10.1016/j.neubiorev.2022.104832.

Lu, Y., Liang, H., Han, D., Mo, Y., Li, Z., Cheng, Y., Xu, X., Shen, Z., Tan, C., Zhao, W., Zhu, Y., Sun, X., 2016. The volumetric and shape changes of the putamen and thalamus in first episode, untreated major depressive disorder. NeuroImage Clin. 11, 658–666. https://doi.org/10.1016/j.nicl.2016.04.008.

MacNiven, K.H., Leong, J.K., Knutson, B., 2020. Medial forebrain bundle structure is linked to human impulsivity. Sci. Adv. 6, eaba4788. https://doi.org/10.1126/sciadv.aba4788.

Maier-Hein, K.H., Neher, P.F., Houde, J.-C., Côté, M.-A., Garyfallidis, E., Zhong, J., Chamberland, M., Yeh, F.-C., Lin, Y.-C., Ji, Q., Reddick, W.E., Glass, J.O., Chen, D.Q., Feng, Y., Gao, C., Wu, Y., Ma, J., He, R., Li, Q., Westin, C.-F., Deslauriers-Gauthier, S., González, J.O.O., Paquette, M., St-Jean, S., Girard, G., Rheault, F., Sidhu, J., Tax, C.M.W., Guo, F., Mesri, H.Y., Dávid, S., Froeling, M., Heemskerk, A.M., Leemans, A., Boré, A., Pinsard, B., Bedetti, C., Desrosiers, M., Brambati, S., Doyon, J., Sarica, A., Vasta, R., Cerasa, A., Quattrone, A., Yeatman, J., Khan, A.R., Hodges, W., Alexander, S., Romascano, D., Barakovic, M., Auría, A., Esteban, O., Lemkaddem, A., Thiran, J.-P., Cetingul, H.E., Odry, B.L., Mailhe, B., Nadar, M.S., Pizzagalli, F., Prasad, G., Villalon-Reina, J.E., Galvis, J., Thompson, P.M., Requejo, F.D.S., Laguna, P.L., Lacerda, L.M., Barrett, R., Dell'Acqua, F., Catani, M., Petit, L., Caruyer, E., Daducci, A., Dyrby, T.B., Holland-Letz, T., Hilgetag, C.C., Stieltjes, B., Descoteaux, M., 2017. The challenge of mapping the human connectome based on diffusion tractography. Nat. Commun. 8, 1349. https://doi.org/10.1038/s41467-017-01285-x.

Malhi, G.S., Mann, J.J., 2018. Depression. Lancet 392, 2299–2312. https://doi.org/10.1016/s0140-6736(18)31948-2.

Markovic, T., Pedersen, C.E., Massaly, N., Vachez, Y.M., Ruyle, B., Murphy, C.A., Abiraman, K., Shin, J.H., Garcia, J.J., Yoon, H.J., Alvarez, V.A., Bruchas, M.R., Creed, M.C., Morón, J.A., 2021. Pain induces adaptations in ventral tegmental area dopamine neurons to drive anhedonia-like behavior. Nat. Neurosci. 24, 1601–1613. https://doi.org/10.1038/s41593-021-00924-3.

Marques, J.P., Kober, T., Krueger, G., van der Zwaag, W., Van de Moortele, P.-F., Gruetter, R., 2010. MP2RAGE, a self bias-field corrected sequence for improved segmentation and T1-mapping at high field. NeuroImage 49, 1271–1281. https://doi.org/10.1016/j.neuroimage.2009.10.002.

McMakin, D.L., Olino, T.M., Porta, G., Dietz, L.J., Emslie, G., Clarke, G., Wagner, K.D., Asarnow, J.R., Ryan, N.D., Birmaher, B., Shamseddeen, W., Mayes, T., Kennard, B., Spirito, A., Keller, M., Lynch, F.L., Dickerson, J.F., Brent, D.A., 2012. Anhedonia predicts poorer recovery among youth with selective serotonin reuptake inhibitor treatment-resistant depression. J. Am. Acad. Child Adolesc. Psychiatry 51, 404–411. https://doi.org/10.1016/j.jaac.2012.01.011.

Mhyre, T.R., Boyd, J.T., Hamill, R.W., Maguire-Zeiss, K.A., 2012. Parkinson's disease. Subcell. Biochem. 65, 389–455. https://doi.org/10.1007/978-94-007-5416-4_16.

Moncrieff, J., Cooper, R.E., Stockmann, T., Amendola, S., Hengartner, M.P., Horowitz, M.A., 2023. The serotonin theory of depression: a systematic umbrella review of the evidence. Mol. Psychiatry 28, 3243–3256. https://doi.org/10.1038/s41380-022-01661-0.

Morales, M., Margolis, E.B., 2017. Ventral tegmental area: cellular heterogeneity, connectivity and behaviour. Nat. Rev. Neurosci. 18, 73–85. https://doi.org/10.1038/nrn.2016.165.

Morris, L.S., Mehta, M., Ahn, C., Corniquel, M., Verma, G., Delman, B., Hof, P.R., Jacob, Y., Balchandani, P., Murrough, J.W., 2022. Ventral tegmental area integrity measured with high-resolution 7-Tesla MRI relates to motivation across depression and anxiety diagnoses. NeuroImage 264, 119704. https://doi.org/10.1016/j.neuroimage.2022.119704.

Mueser, K.T., McGurk, S.R., 2004. Schizophrenia. Lancet Lond. Engl. 363, 2063–2072. https://doi.org/10.1016/S0140-6736(04)16458-1.

Murray, S.B., Cabeen, R.P., Jann, K., Tadayonnejad, R., Strober, M., Feusner, J.D., 2023. White matter microstructure in habit and reward circuits in anorexia nervosa: Insights from a neurite orientation dispersion and density imaging study. Acta Psychiatr. Scand. 147, 134–144. https://doi.org/10.1111/acps.13521.

Novick, J.S., Cook, I.A., Rosenbaum, J.F., Balasubramani, G.K., Rush, A.J., 2005. Clinical and demographic features of atypical depression in outpatients with major depressive disorder: preliminary findings from STAR*D. J Clin Psychiatry.

Oishi, K., Zilles, K., Amunts, K., Faria, A., Jiang, H., Li, X., Akhter, K., Hua, K., Woods, R., Toga, A.W., Pike, G.B., Rosa-Neto, P., Evans, A., Zhang, J., Huang, H., Miller, M.I., van Zijl, P.C.M., Mazziotta, J., Mori, S., 2008. Human brain white matter atlas: Identification and assignment of common anatomical structures in superficial white

matter. NeuroImage 43, 447–457. https://doi.org/10.1016/j.neuroimage.2008.07.009.
Otte, C., Gold, S.M., Penninx, B.W., Pariante, C.M., Etkin, A., Fava, M., Mohr, D.C., Schatzberg, A.F., 2016. Major depressive disorder. Nat Rev Primer 2, 16065. https://doi.org/10.1038/nrdp.2016.65.
Pan, P.M., Sato, J.R., Paillère Martinot, M.-L., Martinot, J.-L., Artiges, E., Penttilä, J., Grimmer, Y., van Noort, B.M., Becker, A., Banaschewski, T., Bokde, A.L.W., Desrivières, S., Flor, H., Garavan, H., Ittermann, B., Nees, F., Papadopoulos Orfanos, D., Poustka, L., Fröhner, J.H., Whelan, R., Schumann, G., Westwater, M.L., Grillon, C., Cogo-Moreira, H., Stringaris, A., Ernst, M., 2022. Longitudinal trajectory of the link between ventral striatum and depression in adolescence. Am. J. Psychiatry 179, 470–481. https://doi.org/10.1176/appi.ajp.20081180.
Pan, P.M., Sato, J.R., Salum, G.A., Rohde, L.A., Gadelha, A., Zugman, A., Mari, J., Jackowski, A., Picon, F., Miguel, E.C., Pine, D.S., Leibenluft, E., Bressan, R.A., Stringaris, A., 2017. Ventral striatum functional connectivity as a predictor of adolescent depressive disorder in a longitudinal community-based sample. Am. J. Psychiatry 174, 1112–1119. https://doi.org/10.1176/appi.ajp.2017.17040430.
Pariyadath, V., Gowin, J.L., Stein, E.A., 2016. Chapter 8 - Resting state functional connectivity analysis for addiction medicine: From individual loci to complex networks, in: Ekhtiari, H., Paulus, M.P. (Eds.), *Progress in Brain Research*, Neuroscience for Addiction Medicine: From Prevention to Rehabilitation - Methods and Interventions. Elsevier, pp. 155–173. https://doi.org/10.1016/bs.pbr.2015.07.015.
Philipsson, J., Sjöberg, R.L., Yelnik, J., Blomstedt, P., 2017. Acute severe depression induced by stimulation of the right globus pallidus internus. Neurocase 23, 84–87. https://doi.org/10.1080/13554794.2017.1284243.
Pizzagalli, D.A., 2022. Toward a better understanding of the mechanisms and pathophysiology of anhedonia: are we ready for translation? Am. J. Psychiatry 179, 458–469. https://doi.org/10.1176/appi.ajp.20220423.
Pizzagalli, D.A., Berretta, S., Wooten, D., Goer, F., Pilobello, K.T., Kumar, P., Murray, L., Beltzer, M., Boyer-Boiteau, A., Alpert, N., El Fakhri, G., Mechawar, N., Vitaliano, G., Turecki, G., Normandin, M., 2019. Assessment of striatal dopamine transporter binding in individuals with major depressive disorder: in vivo positron emission tomography and postmortem evidence. JAMA Psychiatry 76, 854–861. https://doi.org/10.1001/jamapsychiatry.2019.0801.
Plantinga, B., Roebroeck, A., Kemper, V., Uludağ, K., Melse, M., Mai, J., Kuijf, M., Herrler, A., Jahanshahi, A., Romeny, B., Temel, Y., 2016. Ultra-high field MRI post mortem structural connectivity of the human subthalamic nucleus, Substantia Nigra, and Globus Pallidus. Front. Neuroanat 10 (66). https://doi.org/10.3389/fnana.2016.00066.
Polders, D.L., Leemans, A., Hendrikse, J., Donahue, M.J., Luijten, P.R., Hoogduin, J.M., 2011. Signal to noise ratio and uncertainty in diffusion tensor imaging at 1.5, 3.0, and 7.0 Tesla. J. Magn. Reson. Imaging 33, 1456–1463. https://doi.org/10.1002/jmri.22554.
Reddy, P.L., Khanna, S., Subhash, M.N., Channabasavanna, S.M., Rao, B.S., 1992. CSF amine metabolites in depression. Biol. Psychiatry 31, 112–118. https://doi.org/10.1016/0006-3223(92)90198-9.
Rivas-Grajales, A.M., Savadjiev, P., Kubicki, M., Nestor, P.G., Niznikiewicz, M., McCarley, R.W., Westin, C.-F., Shenton, M.E., Levitt, J.J., 2019. Striato-nigro-striatal tract dispersion abnormalities in patients with chronic schizophrenia. Brain Imaging Behav. 13, 1236–1245. https://doi.org/10.1007/s11682-018-9934-9.
Rush, A.J., Gullion, C.M., Basco, M.R., Jarrett, R.B., Trivedi, M.H., 1996. The inventory of depressive symptomatology (IDS): psychometric properties. Psychol. Med. 26, 477–486. https://doi.org/10.1017/s0033291700035558.
Russo, S.J., Nestler, E.J., 2013. The brain reward circuitry in mood disorders. Nat. Rev. Neurosci. 14. https://doi.org/10.1038/nrn3381.
Schapira, A.H.V., Chaudhuri, K.R., Jenner, P., 2017. Non-motor features of Parkinson disease. Nat. Rev. Neurosci. 18, 435–450. https://doi.org/10.1038/nrn.2017.62.
Scheepens, D.S., Waarde, J.A.van, Lok, A., Vries, G.de, Denys, D.A.J.P., Wingen, G.A.van, 2020. The link between structural and functional brain abnormalities in depression: a systematic review of multimodal neuroimaging studies. Front. Psychiatry 11. https://doi.org/10.3389/fpsyt.2020.00485.
Schildkraut, J.J., Gordon, E.K., Durell, J., 1965. Catecholamine metabolism in affective disorders. I. Normetanephrine and VMA excretion in depressed patients treated with imipramine. J. Psychiatr. Res. 3, 213–228. https://doi.org/10.1016/0022-3956(65)90003-8.
Sexton, C.E., Sykara, K., Karageorgiou, E., Zitser, J., Rosa, T., Yaffe, K., Leng, Y., 2019. Connections between insomnia and cognitive aging. Neurosci. Bull. 36, 77–84. https://doi.org/10.1007/s12264-019-00401-9.
Smeets, R.M.W., Dingemans, P., 1993. Composite International Diagnostic Interview (CIDI), Version 1.1. World Health Organ. AmsterdamGeneva.
Smith, R.E., Tournier, J.-D., Calamante, F., Connelly, A., 2015. SIFT2: Enabling dense quantitative assessment of brain white matter connectivity using streamlines tractography. NeuroImage 119, 338–351. https://doi.org/10.1016/j.neuroimage.2015.06.092.
Smith, R.E., Tournier, J.-D., Calamante, F., Connelly, A., 2012. Anatomically-constrained tractography: improved diffusion MRI streamlines tractography through effective use of anatomical information. NeuroImage 62, 1924–1938. https://doi.org/10.1016/j.neuroimage.2012.06.005.
Smith, S.M., Jenkinson, M., Woolrich, M.W., Beckmann, C.F., Behrens, T.E.J., Johansen-Berg, H., Bannister, P.R., De Luca, M., Drobnjak, I., Flitney, D.E., Niazy, R.K., Saunders, J., Vickers, J., Zhang, Y., De Stefano, N., Brady, J.M., Matthews, P.M., 2004. Advances in functional and structural MR image analysis and implementation as FSL. NeuroImage 23 (Suppl 1), S208–S219. https://doi.org/10.1016/j.neuroimage.2004.07.051.
Steinberg, L., 2005. Cognitive and affective development in adolescence. Trends Cogn. Sci. 9, 69–74. https://doi.org/10.1016/j.tics.2004.12.005.
Strotmann, B., Heidemann, R.M., Anwander, A., Weiss, M., Trampel, R., Villringer, A., Turner, R., 2014. High-resolution MRI and diffusion-weighted imaging of the human habenula at 7 tesla. J. Magn. Reson. Imaging 39, 1018–1026. https://doi.org/10.1002/jmri.24252.
Tan, S.K.H., Hartung, H., Schievink, S., Sharp, T., Temel, Y., 2013. High-frequency stimulation of the substantia nigra induces serotonin-dependent depression-like behavior in animal models. Biol. Psychiatry 73, e1–e3. https://doi.org/10.1016/j.biopsych.2012.07.032.
Theisen, F., Leda, R., Pozorski, V., Oh, J.M., Adluru, N., Wong, R., Okonkwo, O., Dean, D.C., Bendlin, B.B., Johnson, S.C., Alexander, A.L., Gallagher, C.L., 2017. Evaluation of striatonigral connectivity using probabilistic tractography in Parkinson's disease. NeuroImage Clin. 16, 557–563. https://doi.org/10.1016/j.nicl.2017.09.009.
Tournier, J.-D., Calamante, F., Connelly, A., 2010. Improved probabilistic streamlines tractography by 2nd order integration over fibre orientation distributions. Proc. Intl. Soc. Mag. Reson. Med. ISMRM 18.
Tournier, J.-D., Smith, R., Raffelt, D., Tabbara, R., Dhollander, T., Pietsch, M., Christiaens, D., Jeurissen, B., Yeh, C.-H., Connelly, A., 2019. MRtrix3: a fast, flexible and open software framework for medical image processing and visualisation. NeuroImage 202, 116137. https://doi.org/10.1016/j.neuroimage.2019.116137.
Travis, A., 2003. Mood disorders, biology (Eds.). In: Aminoff, M.J., Daroff, R.B. (Eds.), Encyclopedia of the Neurological Sciences. Academic Press, New York, pp. 202–208. https://doi.org/10.1016/B0-12-226870-9/01184-9.
Trutti, A.C., Mulder, M.J., Hommel, B., Forstmann, B.U., 2019. Functional neuroanatomical review of the ventral tegmental area. NeuroImage 191, 258–268. https://doi.org/10.1016/j.neuroimage.2019.01.062.
Tustison, N.J., Avants, B.B., Cook, P.A., Zheng, Y., Egan, A., Yushkevich, P.A., Gee, J.C., 2010. N4ITK: improved N3 bias correction. IEEE Trans. Med. Imaging 29, 1310–1320. https://doi.org/10.1109/TMI.2010.2046908.
van Doorn, J., van den Bergh, D., Böhm, U., Dablander, F., Derks, K., Draws, T., Etz, A., Evans, N.J., Gronau, Q.F., Haaf, J.M., Hinne, M., Kucharský, Š., Ly, A., Marsman, M., Matzke, D., Gupta, A.R.K.N., Sarafoglou, A., Stefan, A., Voelkel, J.G., Wagenmakers, E.-J., 2021. The JASP guidelines for conducting and reporting a Bayesian analysis. Psychon. Bull. Rev. 28, 813–826. https://doi.org/10.3758/s13423-020-01798-5.
Veraart, J., Fieremans, E., Novikov, D.S., 2016a. Diffusion MRI noise mapping using random matrix theory. Magn. Reson. Med. 76, 1582–1593. https://doi.org/10.1002/mrm.26059.
Veraart, J., Novikov, D.S., Christiaens, D., Ades-Aron, B., Sijbers, J., Fieremans, E., 2016b. Denoising of diffusion MRI using random matrix theory. NeuroImage 142, 394–406. https://doi.org/10.1016/j.neuroimage.2016.08.016.
Veraart, J., Sijbers, J., Sunaert, S., Leemans, A., Jeurissen, B., 2013. Weighted linear least squares estimation of diffusion MRI parameters: strengths, limitations, and pitfalls. NeuroImage 81, 335–346. https://doi.org/10.1016/j.neuroimage.2013.05.028.
Vrieze, E., Pizzagalli, D.A., Demyttenaere, K., Hompes, T., Sienaert, P., de Boer, P., Schmidt, M., Claes, S., 2013. Reduced reward learning predicts outcome in major depressive disorder. Biol. Psychiatry 73, 639–645. https://doi.org/10.1016/j.biopsych.2012.10.014.
Vu, A.T., Auerbach, E., Lenglet, C., Moeller, S., Sotiropoulos, S.N., Jbabdi, S., Andersson, J., Yacoub, E., Ugurbil, K., 2015. High resolution whole brain diffusion imaging at 7 T for the Human Connectome Project. Neuroimage 122, 318–331.
Wise, R.A., 2009. Roles for nigrostriatal—not just mesocorticolimbic—dopamine in reward and addiction. Trends Neurosci. 32, 517–524. https://doi.org/10.1016/j.tins.2009.06.004.
World Health Organization, 2008. The global burden of disease : 2004 update. World Health Organization.